Optics and Lasers in Engineering 90 (2017) 217–224

Contents lists available at ScienceDirect

Optics and Lasers in Engineering

journal homepage: www.elsevier.com/locate/optlaseng

Superfast 3D absolute shape measurement using five binary patterns

Jae-Sang Hyun, Song Zhang*

School of Mechanical Engineering, Purdue University, West Lafayette, Indiana 47907, USA

ARTICLE INFO

Keywords:
High-speed
Phase-coding
Binary defocusing
Temporal unwrapping

ABSTRACT

This paper presents a method that recovers high-quality 3D absolute coordinates point by point with only five binary patterns. Specifically, three dense binary dithered patterns are used to compute the wrapped phase; and the average intensity is combined with two additional binary patterns to determine fringe order pixel by pixel in phase domain. The wrapped phase is temporarily unwrapped point by point by referring to the fringe order. We further developed a computational framework to reduce random noise impact due to dithering, defocusing and random noise. Since only five binary fringe patterns are required to recover one 3D frame, extremely high speed 3D shape measurement can be achieved. For example, we developed a system that captures 2D images at 3333 Hz, and thus performs 3D shape measurement at 667 Hz.

1. Introduction

High-speed 3D shape measurement using structured light methods has been increasingly employed to capture fast motion due to reduced hardware costs. Yet, it is always beneficial to capture faster motion with the same available hardware technologies.

Typically, a high-speed 3D shape measurement system uses multiple rapidly changing structured patterns to recover one 3D shape. Given a pattern generator, its maximum pattern switching rate is limited by its hardware layout. For example, a now popular digital light processing (DLP) Lightcrafter 4500 can switch binary patterns at 4225 Hz, or 8-bit grayscale patterns at 120 Hz. Therefore, using less number of patterns to recover one 3D shape is always of interest for high-speed applications.

Fourier method uses only a single pattern for 3D shape measurement [1], yet it is limited to measuring rather smooth surfaces without complex texture, and only relative 3D geometry since the phase obtained from such a method is not absolute. To increase its robustness, Guo et al. [2] developed modified FTP method that used two fringe patterns. Though successful, it still can only measure relative shape. Li et al. [3] added one more pattern to determine fringe order for 3D absolute shape measurement. However, this method requires the voting process for fringe order determination, making it difficult to measure object with complex surface geometry. Furthermore, comparing with phase-shifting method, the phase accuracy obtained from the Fourier method is much lower. Therefore, for high accuracy measurements, phase-shifting methods are preferable.

By encoding one single marker on carried fringe patterns, Zhang et al. [4] recovered absolute phase only using three phase-shifted fringe patterns. Similarly, Cui et al. [5] developed absolute recovery method by encoding a single line on three phase-shifted fringe patterns. These marker encoding methods work if the surface geometry is smooth since a spatial phase unwrapping algorithm is required.

Methods also developed to recover absolute phase by adding a second camera. Li et al. [6] developed a method to obtain absolute phase with three phase-shifted fringe patterns by using geometric constraint for a dual-camera and a single projector system. Lohry and Zhang [7] developed two-stage method that uses stereo camera to obtain rough disparity map and uses phase to refine the disparity map. Despite some advantages, these techniques use two cameras and one projector. Such a dual-camera and a single projector technique creates more shadow related problems since all three devices must see the point in order to measure the point. Moreover, the high-speed cameras are usually very expensive. Therefore, using a single projector and a single camera for high-speed measurements is still desirable.

For absolute phase measurement, it typically requires more than three fringe patterns for a single-projector and a single-camera system. Liu et al. [8] developed a method that uses five phase-shifted fringe patterns by compositing two-frequency phase information into the same phase-shifted patterns, and the absolute phase is recovered after demodulating the phase. Zuo et al. [9] applied a similar strategy using binary defocusing method with tripolar pulse-width-modulation (TPWM) for kHz 3D shape measurement. However, since these methods encode two frequency phases into the same fringe pattern, the phase-quality is compromised compared to the single frequency phase encoding methods.

* Corresponding author.
E-mail address: szhang15@purdue.edu (S. Zhang).

http://dx.doi.org/10.1016/j.optlaseng.2016.10.017
Received 14 July 2016; Received in revised form 13 October 2016; Accepted 14 October 2016

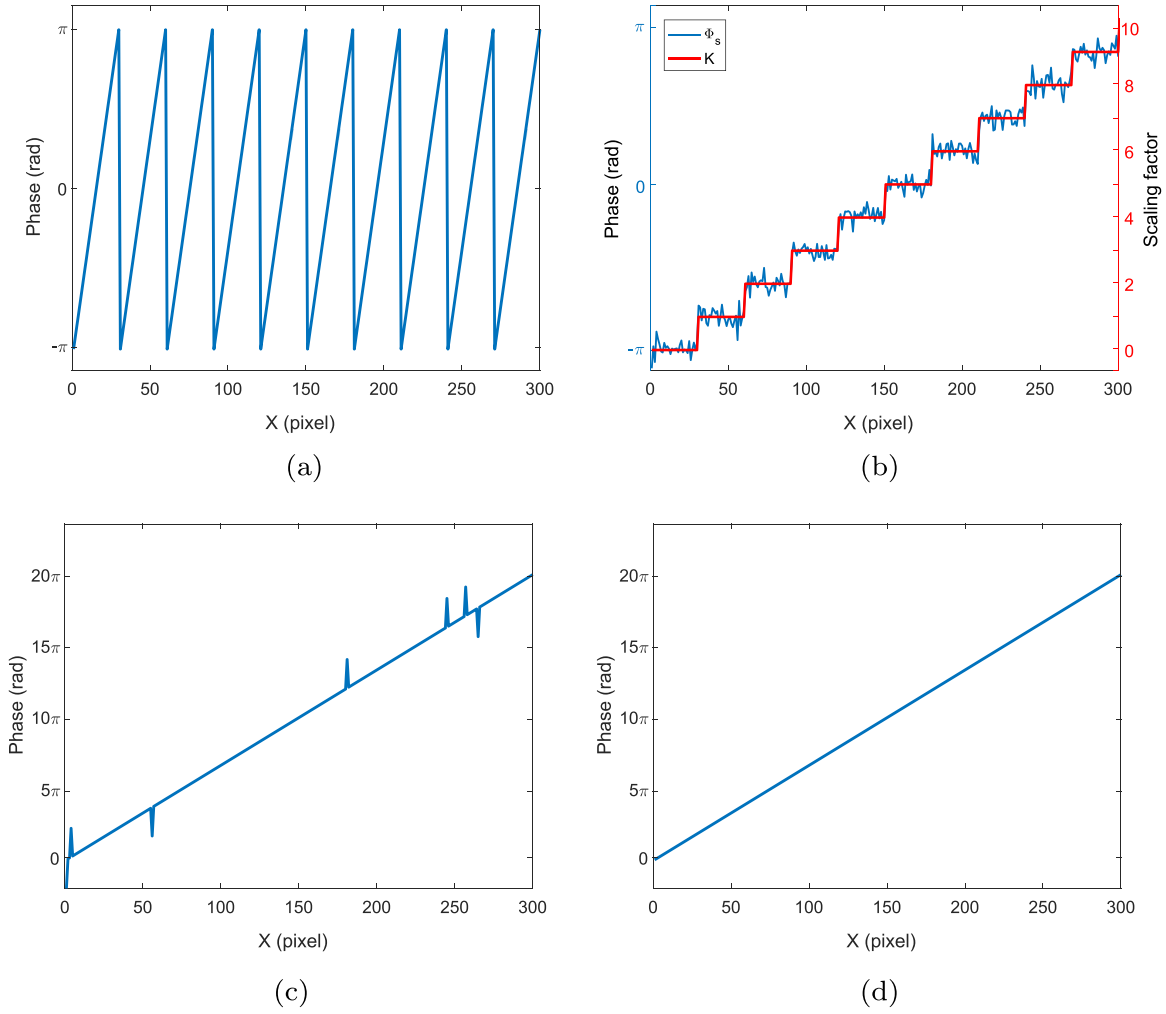

Fig. 1. Cross section of ideal image. (a) Wrapped phase map with fringe period of 30 pixels; (b) comparison of the stair phase with the fringe order after rounding off the phase to the nearest integer; (c) absolute phase directly obtained from Eq. (11); (d) absolute phase after removing spikes.

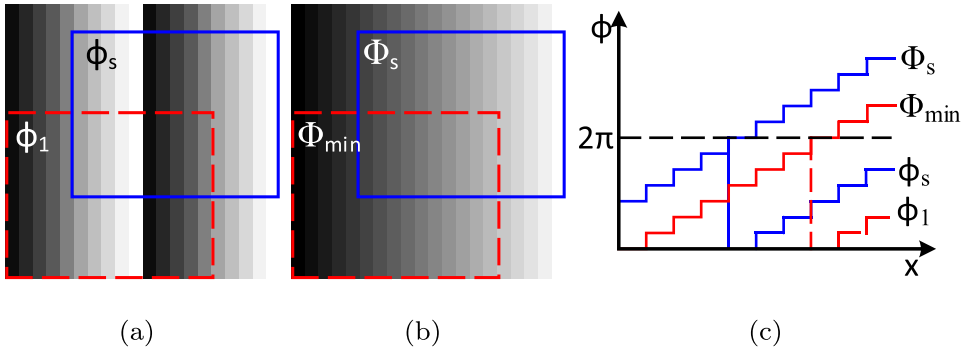

Fig. 2. Conceptual idea of removing 2π discontinuity of stair phase map by using the minimum phase. (a) Wrapped stair phase map by using Eq. (10); (b) unwrapped stair phase map after adding 2π where discontinuity occurs; (c) cross section of Φ_{min} and Φ_s and the wrapped phase maps. (For interpretation of the references to color in this figure, the reader is referred to the web version of this article.)

It is well known that absolute phase can be obtained by using two sets of phase-shifted fringe patterns with two different frequencies with the equivalent wavelength to cover the whole range of sensing [10]; and for digital fringe projection (DFP) systems, one can also use a wide fringe pattern with a single period of sinusoidal pattern covering the whole range [11]. Yet, due to noise, it is typically difficult for two-wavelength methods to choose very narrow fringe patterns for higher frequency phase [12].

For DFP systems, one can also combine binary patterns with phase-shifted fringe patterns for absolute phase recovery [13]. In essence, this hybrid method uses the binary patterns to determine fringe order for each pixel and unwrap the absolute phase. However, three binary patterns can only generate 8 unique numbers, and thus this method cannot use more than 8 fringe stripes if only six patterns are used. Wang and Zhang [14] proposed a method that encodes fringe order information into the phase of three phase-shifted fringe patterns for absolute phase unwrapping. Such a method has proven successful to use narrow fringe patterns with only six patterns. Yet, these methods use one more pattern for absolute phase retrieval than those methods only using five patterns [8,9]. To retrieve more accurate absolute phase

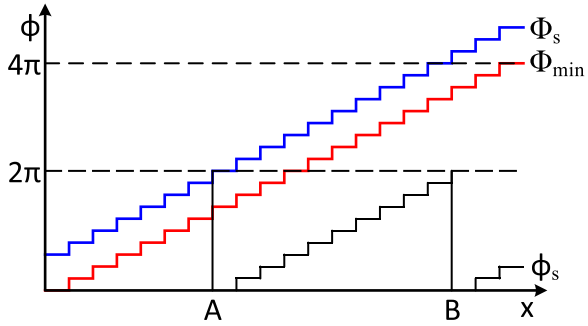

Fig. 3. Determination of the number of 2π jumps of the stair phase over two periods.

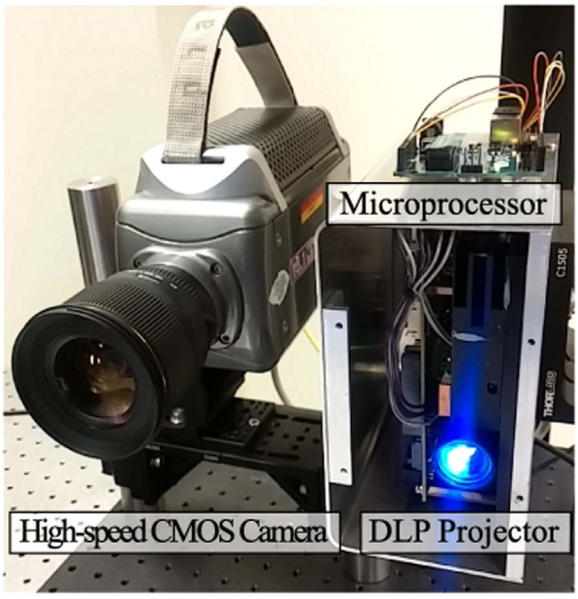

Fig. 4. Experimental setup for DFP calibration.

with higher frequency, Zheng et al. [15] proposed to use six additional patterns to encode fringe order; though successful, it actually increases the number of patterns used (9 total patterns). Apparently, similar concepts can be implemented into three color channels [16], but it is well known that using color is not desirable to measure colorful object. Lately, Xing et al. [17] attempted to use the Newton–Raphson method to address the nonlinear gamma issues of the phase-coding method if the projector's nonlinear gamma is not pre-calibrated.

The above mentioned phase-coding methods all use 8-bit patterns for phase recovery, which is good for slow speed applications. Yet, to capture higher speed motions, faster 3D shape measurement is required. If binary patterns are used, much higher frame rates (kHz) can be achieved especially when a DLP projector is used. This paper presents a method that only uses five binary fringe patterns for pixel-by-pixel and dense absolute phase recovery. Specifically, three dense binary dithered patterns are used to compute the wrapped phase; and the average intensity and two additional binary patterns are used to determine fringe order pixel by pixel in phase domain using the phase-coding method developed by Wang and Zhang [14]. The wrapped phase is temporarily unwrapped point by point by referring to the fringe order. To use narrow fringe patterns and reduce noise impact, we further developed a computational framework by using geometric constraint of the DFP system. Since only binary patterns are required, we demonstrated that superfast 3D shape measurement can be achieved: we developed a system that can capture binary patterns at 3333 Hz; and since 5 patterns can recover one 3D shape, we achieved a 667 Hz 3D shape measurement rate.

Section 2 discusses the principles behind the proposed method. Section 3 presents experimental validation; and Section 4 summarizes this paper.

2. Principle

In this section, we introduce related theoretical background of this research. Phase-shifting algorithm is briefly introduced, and the proposed five pattern absolute phase unwrapping method is detailed, and the proposed computational framework is elucidated.

2.1. Three-step phase-shifting algorithm

Over recent decades, a number of strategies for phase-shifting algorithm that are widely known in the field of 3D optical metrology have been rapidly improved. Phase-shifting methods have considerable advantages: robust to noise and surface reflectivity variations, and accurate in pixel-by-pixel 3D coordinate reconstruction. Among all phase-shifting algorithms, the three-step phase-shifting algorithm requires minimum number of fringe patterns for phase calculation. Three patterns can be mathematically described as,

$$I_1(x,y) = I'(x,y) + I''(x,y)\cos[\phi(x,y) - 2\pi/3], \tag{1}$$

$$I_2(x,y) = I'(x,y) + I''(x,y)\cos[\phi(x,y)], \tag{2}$$

$$I_3(x,y) = I'(x,y) + I''(x,y)\cos[\phi(x,y) + 2\pi/3], \tag{3}$$

where $I'(x,y)$ is the average intensity, $I''(x,y)$ the intensity modulation, and $\phi(x,y)$ the phase to be solved for. By means of using an inverse tangent function, the phase can be easily described as,

$$\phi(x,y) = \tan^{-1}\left[\frac{\sqrt{3}(I_1 - I_3)}{2I_2 - I_1 - I_3}\right]. \tag{4}$$

Because of the limitation of the arctangent function, the phase obtained from Eq. (4) ranges from $-\pi$ to $+\pi$. To retrieve absolute phase, a temporal phase-unwrapping framework is usually needed. In the next section, we will introduce our proposed temporal phase unwrapping method. Phase unwrapping essentially determines fringe order $K(x,y)$ such that 2π discontinuities of the wrapped phase can be properly unwrapped

$$\Phi(x,y) = 2\pi \times K(x,y) + \phi(x,y), \tag{5}$$

Here $\Phi(x,y)$ denotes the unwrapped phase map.

Eqs. (1)–(3) also give the average intensity information as

$$I'(x,y) = [I_1(x,y) + I_2(x,y) + I_3(x,y)]/3, \tag{6}$$

which can be used to determine the texture of the object.

2.2. Proposed phase-coding algorithm

We propose a new method that only requires two additional patterns to determine fringe order for each pixel, these two additional fringe patterns directly encode fringe order information as,

$$\Phi_s(x,y) = -\pi + Floor[x/T] \times \frac{2\pi}{N}, \tag{7}$$

$$I_4(x,y) = I'(x,y) + I''(x,y)\cos[\Phi_s(x,y)], \tag{8}$$

$$I_5(x,y) = I'(x,y) + I''(x,y)\sin[\Phi_s(x,y)], \tag{9}$$

where Φ_s is the stair phase map which determines the fringe order depending on where (x,y) is located, N is the number of stairs, $Floor[]$ is the floor operator to determine the truncated integer number, and T is the fringe pitch, number of pixels per fringe period. In this case, there are 3 unknowns (I', I'', and Φ_s) and 2 equations (Eqs. (8) and (9)). To uniquely solve for Φ_s and thus fringe order, we combine Eq. (6) with these two equations. $\Phi_s(x,y)$ and fringe order $K(x,y)$ can be uniquely solved for each pixel as,

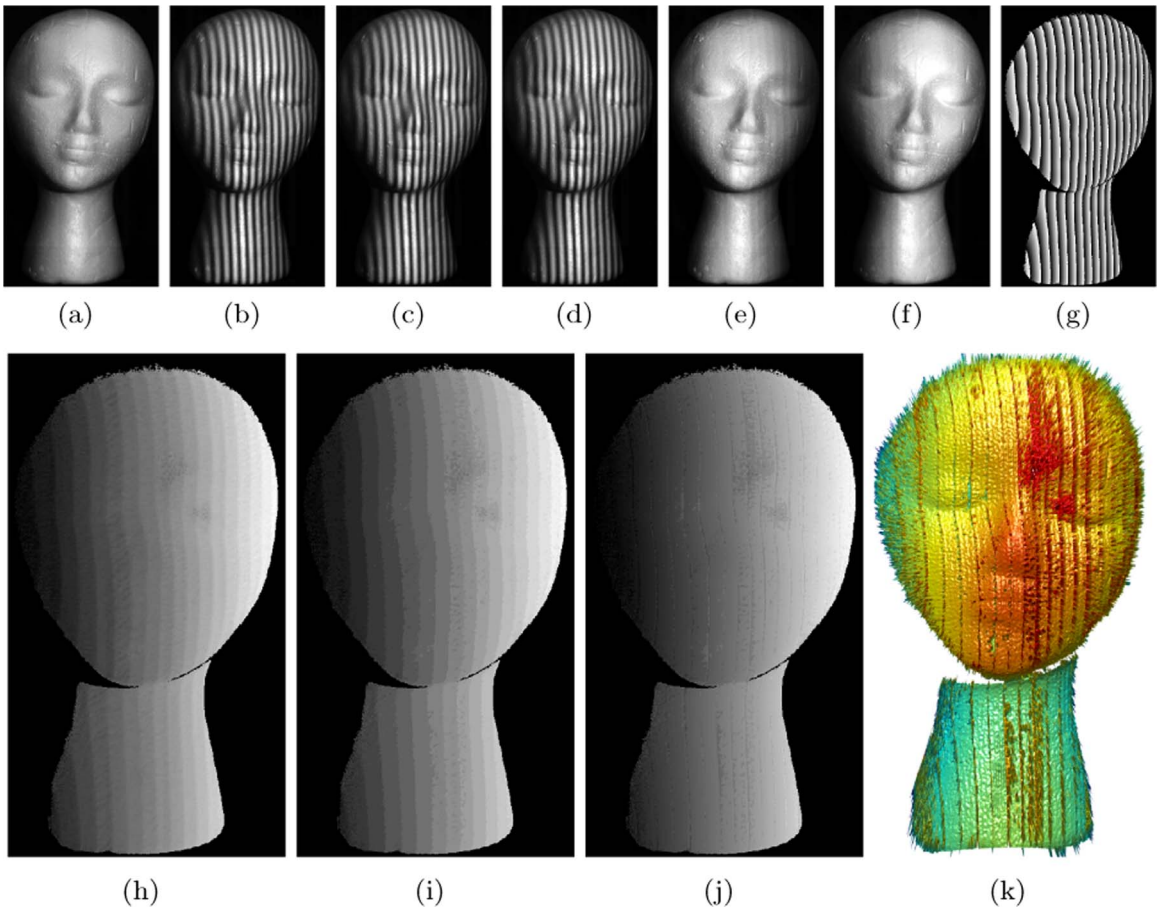

Fig. 5. Experimental captured data of the proposed method with a fringe period of 1140 pixels for the stair phase. (a) Photograph of the measured statue; (b)–(d) three phase-shifted high-frequency fringe images; (e)–(f) two phase-shifted low-frequency fringe images; (g) wrapped phase from high-frequency fringe patterns; (h) absolute stair phase map Φ_s; (i) fringe order map K; (j) unwrapped phase Φ; (k) 3D reconstruction result.

$$\Phi_s(x, y) = \tan^{-1}\left[\frac{I_5 - I'}{I_4 - I'}\right], \tag{10}$$

$$K(x, y) = Round\left[N \times \left(\frac{\Phi_s + \pi}{2\pi}\right)\right]. \tag{11}$$

It should be noted that $\Phi_s(x, y)$ is the unwrapped phase since one single fringe pattern covers the whole fringe span.

Fig. 1 shows an example of using the proposed temporal phase unwrapping method. Fig. 1(a) shows the wrapped phase from three phase-shifted fringe patterns. Fig. 1(b) shows the wrapped phase before quantization and the integer number of the fringe order. In this example, Gaussian noise with a signal to noise ratio (SNR) of 25 was added to fringe patterns to emulate the practical system noise. Fig. 1(c) shows the result after directly applying the fringe order to temporally unwrap the wrapped phase pixel-by-pixel. One can clearly see spiky noise on the unwrapped phase map. Such spiky noise can be reduced by applying a computational framework such as a median filter. Fig. 1(d) shows the result after the computational framework discussed by Karpinsky et al. [18].

Our experimental data shows that if the noise is larger and/or the phase shifted fringe patterns are narrower (i.e., more stairs are used), the aforementioned computational framework fails to effectively reduce the spiky noise. Unfortunately, for our high-speed measurement application, the noise is quite large and we have to use narrow fringe pattern to achieve high-quality measurement. To address this problem, we have developed an computational framework to significantly reduce noise impact, which will be discussed next.

2.3. Computational framework for reducing noise influence

As aforementioned, to achieve high accuracy, the fringe period needs to be small, and thus the encoded stair height is small, making it more sensitive to noise; and the use of dithered pattern and out-of-focus projector further deteriorates fringe quality. To address such problems, we propose to use the geometric constraints of the DFP system to allow the use of more than one period of patterns (i.e., more than 2π phase range) to encode fringe order. This section details the principle of this computational approach.

To understand the proposed method, DFP system geometric model needs to be discussed. In this research, we utilize the well-known pinhole model to illustrate the imaging lenses of a DFP system. The model mathematically describes the relationship between 3D (x^w, y^w, z^w) world coordinates and 2D (u, v) imaging coordinates as,

$$s\begin{bmatrix} u \\ v \\ 1 \end{bmatrix} = \begin{bmatrix} f_u & \gamma & u_0 \\ 0 & f_v & v_0 \\ 0 & 0 & 1 \end{bmatrix}\begin{bmatrix} r_{11} & r_{12} & r_{13} & t_1 \\ r_{21} & r_{22} & r_{23} & t_2 \\ r_{31} & r_{32} & r_{33} & t_3 \end{bmatrix}\begin{bmatrix} x^w \\ y^w \\ z^w \\ 1 \end{bmatrix}, \tag{12}$$

where s is a scaling factor; f_u and f_v are, respectively, the effective focal length in u and v directions; γ is the skew factor of u and v axes, and for research-grade cameras γ=0; r_{ij} and t_i, respectively, denote the rotation and translation variables; and (u_0, v_0) is the principle point. We can simplify the matrices as,

$$\mathbf{P} = \begin{bmatrix} f_u & \gamma & u_0 \\ 0 & f_v & v_0 \\ 0 & 0 & 1 \end{bmatrix}\begin{bmatrix} r_{11} & r_{12} & r_{13} & t_1 \\ r_{21} & r_{22} & r_{23} & t_2 \\ r_{31} & r_{32} & r_{33} & t_3 \end{bmatrix} = \begin{bmatrix} p_{11} & p_{12} & p_{13} & p_{14} \\ p_{21} & p_{22} & p_{23} & p_{24} \\ p_{31} & p_{32} & p_{33} & p_{34} \end{bmatrix}, \tag{13}$$

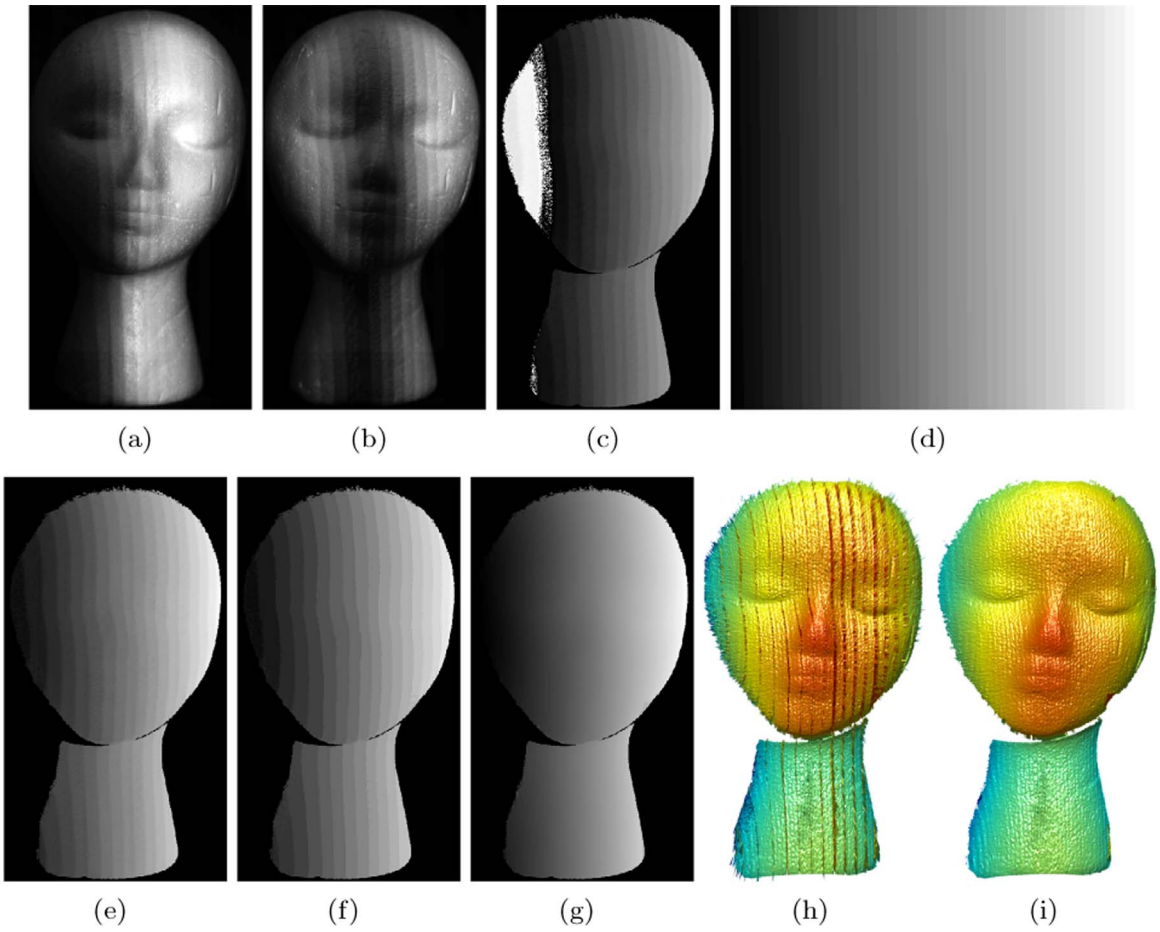

Fig. 6. Experimental captured data of the proposed method using geometric constraints. (a)–(b) two stair-shaped patterns (I_4 and I_5) for ϕ_s with a fringe period of 570 pixels; (c) wrapped stair phase ϕ_s with a 2π discontinuity; (d) the artificial minimum phase map when $z = z_{min}$; (e) unwrapped stair phase Φ_s using the geometric constraints; (f) fringe order map K; (g) unwrapped phase Φ; (h) 3D reconstruction result using the proposed method without applying any filter; (i) filtered 3D reconstruction result.

where the projection matrix P can be estimated through calibration. The projector and the camera have exactly the same mathematical model, albeit the projector is an output device, as the inverse of a camera. If both projector and camera are calibrated under the same world coordinate system, we have

$$s^p [u^p \;\; v^p \;\; 1]^t = P^p [x^w \;\; y^w \;\; z^w \;\; 1]^t, \tag{14}$$

$$s^c [u^c \;\; v^c \;\; 1]^t = P^c [x^w \;\; y^w \;\; z^w \;\; 1]^t. \tag{15}$$

Here superscript p denotes the projector, superscript c the camera, and superscript t the transpose of a matrix. Eqs. (14) and (15) have six equations and seven unknowns (s^c, s^p, x^w, y^w, z^w, u^p, v^p) for a given camera pixel (u^c, v^c). Therefore, we need one more equation to solve for u^p to get the corresponding absolute phase, which can be obtained by the linear relationship between absolute phase Φ and u^p,

$$u^p = \Phi \times T/(2\pi), \tag{16}$$

where T is a projection patterns fringe period in pixel. For any given point, if z is known, the corresponding points for each camera pixel, (u^c, v^c), can computed and thus the phase value can be determined,

$$\Phi(u^c, v^c) = f(z, T, P^c, P^p). \tag{17}$$

Assume that $z = z_{min}$ which is the minimum depth z for the volume of interest, the virtual absolute phase map, Φ_{min}, corresponding to z_{min} can be generated by using Eq. (17). We call Φ_{min} as the minimum phase. Under the circumstance, Eq. (10) only yields wrapped phase map $\phi_s = \Phi_s \bmod (2\pi)$ since more than one period of fringe patterns are used. Since ϕ_s is calculated by simply using Eq. (10), the measurement volume is restricted as discussed by An et al. [19]. The wrapped phase can be unwrapped pixel-by-pixel by comparing Φ_{min} to obtain absolute phase Φ_s.

Fig. 2 illustrates the fundamental concept of using the minimum phase to unwrapped periodical stair phase. Fig. 2(a) shows the wrapped stair phase map with two periods of fringe patterns. The red dashed windows is the wrapped stair phase map of ϕ_1 when $z = z_{min}$ and the blue window is the phase map of ϕ_s when $z > z_{min}$. Fig. 2(b) shows the phase map of Φ_{min}. This figure shows that the absolute phase Φ_s can be obtained by adding 2π when $\Phi_{min} > \phi_s$, as illustrated in Fig. 2(c).

Fig. 3 shows a case for three periodical fringe patterns. If ϕ_s is located between the point A and B, the difference between Φ_{min} and ϕ_s is greater than zero and less than 2π. Then, 2π should be added on the region. If ϕ_s is located on the right of the point B, 4π should be added to get a correct fringe order map. In other words, if the stair phase satisfies the following condition for an integer number P,

$$2\pi \times (P-1) < \Phi_{min} - \phi_s < 2\pi \times P, \tag{18}$$

or

$$P(x, y) = Ceil\left[\frac{\Phi_{min}(x, y) - \phi_s(x, y)}{2\pi}\right], \tag{19}$$

the absolute stair phase Φ_s can be determined as

$$\Phi_s(x, y) = 2\pi \times P(x, y) + \phi_s(x, y), \tag{20}$$

and fringe order K as

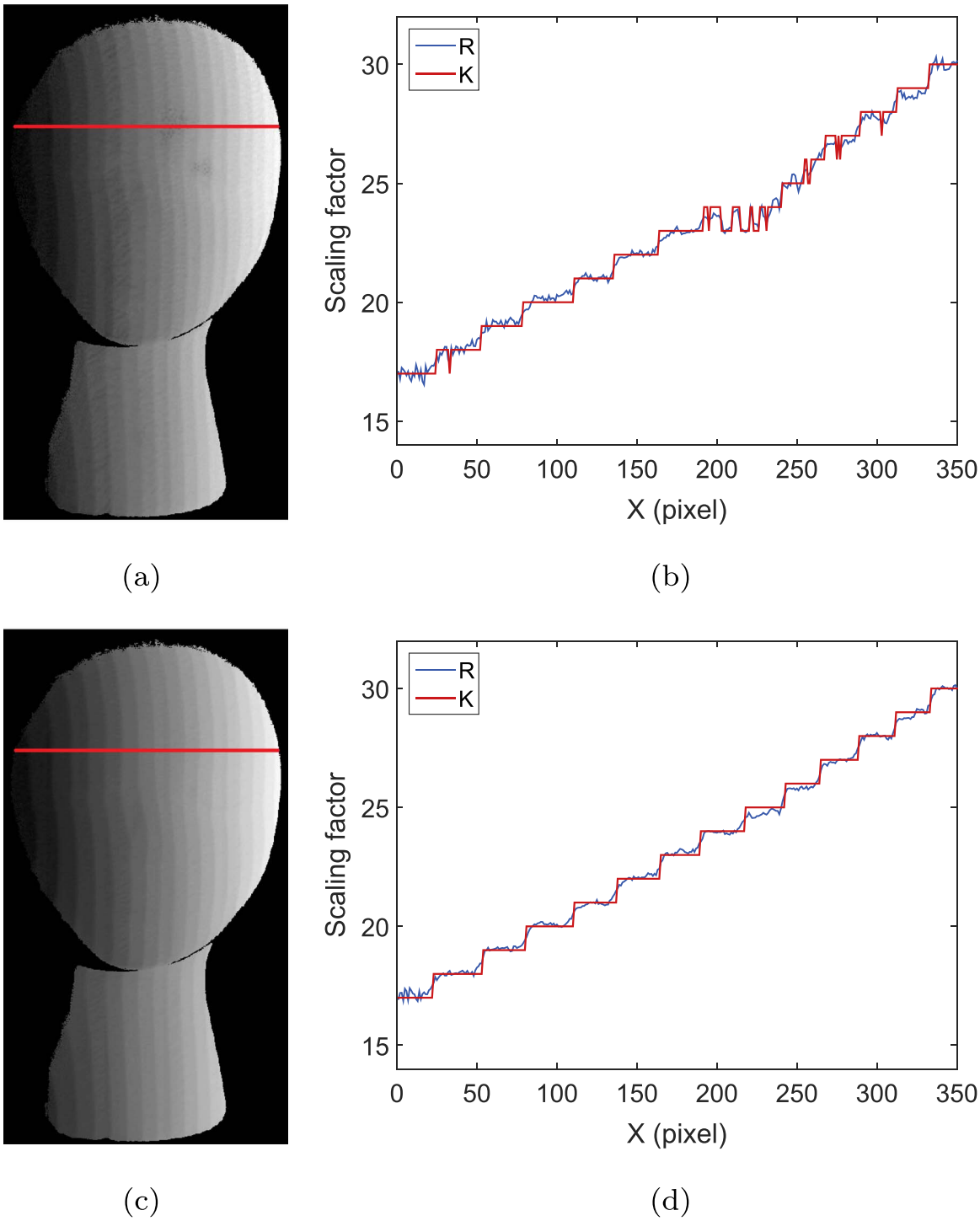

Fig. 7. Images of the stair phase and graphs of a cross section to compare the real number with its quantized number. (a) Absolute stair phase map by using the conventional method; (b) cross section of the red line on (a) to describe R and corresponding K of the conventional method; (c) absolute stair phase map by using the proposed method; (d) cross section of the red line on (c) to describe R and corresponding K of the proposed method. (For interpretation of the references to color in this figure legend, the reader is referred to the web version of this article.)

$$K(x, y) = Round\left[M \times \left(\frac{\Phi_s(x, y) + \pi}{2\pi}\right)\right], \tag{21}$$

where $Ceil[]$ is the ceiling operator that gives the closest upper integer number, and M is the number of stairs in one period of the stair phase. We can simplify Eq. (21) as

$$R(x, y) = M \times \left[\frac{\Phi_s(x, y) + \pi}{2\pi}\right], \tag{22}$$

and

$$K(x, y) = Round[R(x, y)], \tag{23}$$

where $R(x, y)$ is the real number to determine the integer number of fringe order K.

In summary, the proposed computational framework can more robustly unwrap the phase by allowing the use of more than one period of fringe patterns to encode stair phase map. The key idea is to artificially create a minimum phase map using geometric constraints of

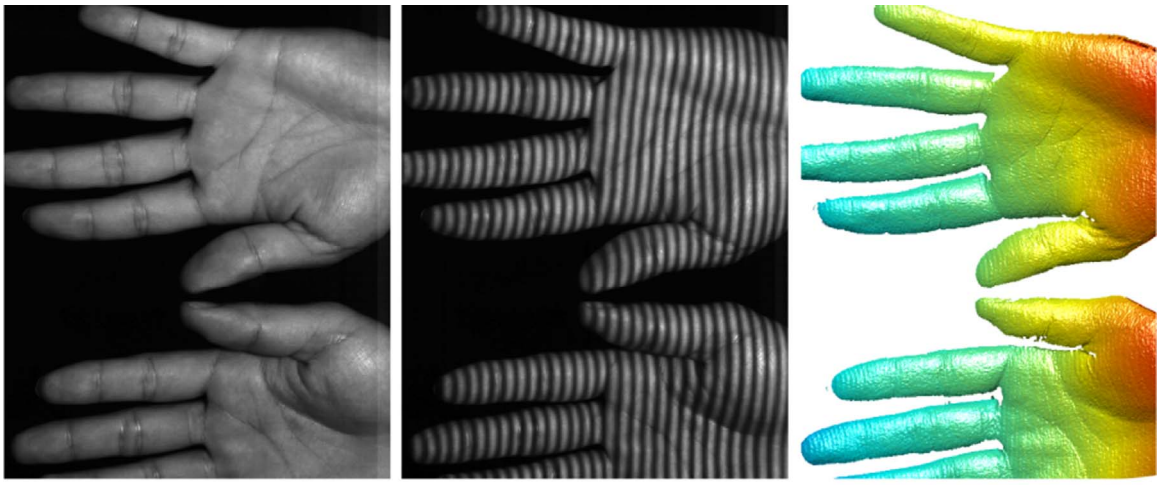

Fig. 8. Measurement result of capturing hands in high-speed (associate Video: https://engineering.purdue.edu/ZhangLab/videos/OLE_Hyun_2016_Video.mp4. (a) Photograph of two hands; (b) one of three phase-shifted fringe patterns; (c) 3D reconstruction result.

the DFP system. The minimum phase map then unwraps the periodical stair phase map. Once the periodical stair phase is unwrapped, fringe order K can be determined that can be further used to temporally unwrap the wrapped phase. Because the proposed method allows the use of more than one period of fringe patterns for stair phase encoding, it is more robust to noise, enabling the use of narrower fringe patterns for higher accuracy measurement.

3. Experiments

A hardware system was developed to verify the performance of the proposed method. Fig. 4 shows the photograph of our system. The system consists of a complementary metal oxide semiconductor (CMOS) camera (Model: Vision Research Phantom V9.1), a digital light processing (DLP) projector (Model: Texas Instruments LightCrafter 4500) and a microprocessor (Model: Arduino Uno). The camera is attached with a lens (Model: SIGMA 24 mm f/1.8 EX DG) whose focal length is 24 mm and aperture ranges from f/1.8 to f/22. The projector has the resolution of 912 × 1140 pixels. The microprocessor is utilized to synchronize the camera with the projector. The system is calibrated using the method developed by Li et al. [20].

We first measured a statue with the proposed method. Fig. 5 shows the results. In this experiment, the camera resolution was set as 1024 × 1024 pixels, and the projector sequentially projects five binary dithered patterns at 1 kHz, and the camera precisely synchronized with the projector captures each projected patterns. The phase-shifted fringe patterns have a fringe period of 30 pixels, and the stair phase encoded patterns have a fringe period of 1140 pixels. Fig. 5(a) shows the image of the sculpture. We cropped all images in a same way for better visualization. Fig. 5(b)-–(f) show five captured fringe patterns. From three phase-shifted fringe patterns shown in Fig. 5(b)–(d), we computed the wrapped phase map, as shown in Fig. 5(g). Combining the averaged image, $I'(x, y)$, with two additional fringe patterns shown in Fig. 5(e)–(f), we obtained the stair phase map $\Phi_s(x, y)$ as shown in Fig. 5(h). The fringe order of the wrapped phase can be calculated by using Eq. (11). Fig. 5(i) shows the fringe order map. Once fringe order is determined, the phase can be unwrapped pixel by pixel. Fig. 5(j) shows the unwrapped phase map. Due to the dithering effect and random noise of the system, the spiky noise is very severe. To visualize such a problem, we recovered 3D geometry of the object from the unwrapped phase. Fig. 5(k) shows the result. It is obvious that it is very difficult to remove all spiky noise by filtering.

In comparison, we employed our proposed method to encode the stair phase. Instead of using one single fringe period, we used 2 periodical fringe patterns. Fig. 6(a)–(b) show those two fringe patterns. The phase map obtained by directly applying Eq. (10) is shown in Fig. 6(c), which still has 2π discontinuities, as expected. We then generated the minimum phase map Φ_{min}, as shown in Fig. 6(d), that was further used the unwrap the stair phase map. Fig. 6(e) shows the unwrapped stair phase map using the proposed method. This stair phase map is then used to generate fringe order map, shown in Fig. 6(f), and temporally unwrap the phase map shown in Fig. 6(g). Fig. 6(h) shows the reconstructed 3D shape. Compared with the result shown in Fig. 5(k), the spiky noise is substantially reduced, which can then be further removed by applying the computational framework developed by Karpinsky et al. [18]. Fig. 6(i) shows the final result, which is fairly smooth, proving that the proposed method can successfully recover 3D shape of an object.

To show the difference between the proposed method and the conventional method clearly, we compared one cross section of the data. R was computed using Eq. (22), from which fringe order can bed determined using Eq. (23). Fig. 7(a) and (c) respectively show Φ_s using the conventional method and the proposed method. The red line describes the region where the cross section is to be compared. Fig. 7(b) shows the graph of R and corresponding integer number K in the conventional method. In the middle of the graph, the noise become severe and the fringe order fluctuates depending on the noise effect. In comparison, R in Fig. 7(d) which is obtained from the proposed computational framework is stable enough to determine the fringe order correctly. Despite some fluctuating noise, fringe order can still be correct correctly obtained. These two graphs verify that the proposed method is more robust to determine fringe order.

To demonstrate the capability of high-speed 3D shape measurement and absolute phase recovery, we simultaneously measured tow moving hands. In this experiment, we set the camera resolution as 672 × 768. The projector projects and the camera captures at 3333 Hz with an exposure time of 300 μs. Since five images are used to recover one 3D geometry, 3D measurement speed is actually 667 Hz. Fig. 8 shows the measurement results. Fig. 8(a) shows one of the frames we captured, and Fig. 8(b) shows one of the fringe patterns for that frame. Fig. 8(c) and associated video (Link: https://engineering.purdue.edu/ZhangLab/videos/OLE_Hyun_2016_Video.mp4) shows the sequence results for this experiment. This experiment successfully demonstrated that our proposed method can measure multiple isolated objects at high speed.

4. Summary

This paper has presented a superfast 3D absolute shape measurement method using five binary patterns. The proposed method uses binary dithering technique for high speed image projection, and reduces the number of frames by using the average intensity. We demonstrated that the noise of patterns due to dithering and random noise can be substantially reduced with the computational framework we developed. Our experimental results demonstrated that high-quality 3D shape measurement can be realized at a speed of 667 Hz.

Acknowledgments

This study was sponsored by the National Science Foundation, USA under grant numbers CMMI-1531048. The views expressed in this paper are those of the authors and not necessarily those of the NSF.

References

[1] Takeda M, Mutoh K. Fourier transform profilometry for the automatic measurement of 3-d object shapes. Opt Express 1983;22(24):3977–82.
[2] Guo L, Su X, Li J. Improved fourier transform profilometry for the automatic measurement of 3d object shapes. Opt Eng 1990;29(12):1439–44.
[3] Li Y, Zhao C, Qian Y, Wang H, Jin H. High-speed and dense three-dimensional surface acquisition using defocused binary patterns for spatially isolated objects. Opt Express 2010;18(21):21628–35.
[4] Zhang S, Yau S-T. High-resolution, real-time 3-d absolute coordinate measurement based on a phase-shifting method. Opt Express 2006;14(7):2644–9.
[5] Cui H, Liao W, Dai N, Cheng X. A flexible phase-shifting method with absolute phase marker retrieval. Measurement 2012;45:101–8.
[6] Li Z, Zhong K, Li YF, Zhou X, Shi Y. Multiview phase shifting: a full-resolution and high-speed 3d measurement framework for arbitrary shape dynamic objects. Opt Lett 2013;38(9):1389–91.
[7] Lohry W, Chen V, Zhang S. Absolute three-dimensional shape measurement using coded fringe patterns without phase unwrapping or projector calibration. Opt Express 2014;22(2):1287–301.
[8] Liu K, Wang Y, Lau DL, Hao Q, Hassebrook LG. Dual-frequency pattern scheme for high-speed 3-d shape measurement. Opt Express 2010;18(5):5229–44.
[9] Zuo C, Chen Q, Gu G, Feng S, Feng F, Li R, Shen G. High-speed three-dimensional shape measurement for dynamic scenes using bi-frequency tripolar pulse-width-modulation fringe projection. Opt Lasers Eng 2013;51(8):953–60.
[10] Cheng Y-Y, Wyant JC. Two-wavelength phase shifting interferometry. Appl Opt 1984;23(24):4539–43.
[11] Wang Y, Zhang S. Superfast multifrequency phase-shifting technique with optimal pulse width modulation. Opt Express 2011;19(6):5143–8.
[12] Creath K. Step height measurement using two-wavelength phase-shifting interferometry. Appl Opt 1987;26(14):2810–6.
[13] Wang Y, Zhang S, Oliver JH. 3-d shape measurement technique for multiple rapidly moving objects. Opt Express 2011;19(9):5149–55.
[14] Wang Y, Zhang S. Novel phase coding method for absolute phase retrieval. Opt Lett 2012;37(11):2067–9.
[15] Zheng D, Da F. Phase coding method for absolute phase retrieval with a large number of codewords. Opt Express 2012;20(22):24139–50.
[16] Li B, Fu Y, Zhang J, Wu H, Xia G, Jiang G. A fast three-dimensional shape measurement method based on color phase coding. Opt Int J Light Electron Opt 2016;127(3):1011–5.
[17] Xing Y, Quan C, Tay C. A modified phase-coding method for absolute phase retrieval. Opt Lasers Eng.
[18] Karpinsky N, Hoke M, Chen V, Zhang S. High-resolution, real-time three-dimensional shape measurement on graphics processing unit. Opt Eng 2014;53(2):024105.
[19] An Y, Hyun J-S, Zhang S. Pixel-wise absolute phase unwrapping using geometric constraints of structured light system. Opt Express 2016;24(16):18445–59.
[20] Li B, Karpinsky N, Zhang S. Novel calibration method for structured-light system with an out-of-focus projector. Appl Opt 2014;53(16):3415–26.